Research article　　　　　　　　　　　　　　　　　　　　　　　　**Open Access**

Optimum Concentrate Stream Concentration in CaCl$_2$ Removal from Sugar Solution Using Electrodialysis

Jogi Ganesh Dattatreya Tadimeti, Anusha Chandra and Sujay Chattopadhyay*

Polymer and Process Engineering Department, I.I.T.Roorkee, SRE Campus, UP-247 001, India

Abstract

Batch electrodialysis (ED) with continuous recirculation was carried out to remove CaCl2 from sugar solution at room temperature. Role of limiting process parameters e.g. (i) concentrate concentration, (ii) sugar mass% cum solution viscosity and (iii) ionic conductivity on electrolyte removal rate were investigated. Unsteady state mass balance defining ion transport through the ED cell with its initial and boundary conditions were solved with linearized Nernst-Planck equation. A new Sherwood number expression appropriate to the cell geometry and process parameters (physical properties and conductivity ratios) is developed as $Sh = a.Re^b.Sc^c \left(\frac{\dot{E}_{Dil}}{\dot{E}_{Conc}} \right)^d$ to estimate mass transfer coefficients and ionic flux. Electrolyte removal percentage can't be correctly estimated from ED cell current instead model based estimates of the flux components due to concentration gradient (chemical potential) and applied electric potential could closely predict the experimental data on electrolyte removal. The ratios of electrolytes removal rates (with and without sugar) can be expressed as power function of viscosity ratios as $\frac{percentremoval_c}{percentremoval_{DSC}} = \left(\frac{\mu_{DSC}}{\mu_C} \right)^{0.28}$. This factor of 0.28~0.3 resembles close similarity with Sc number in the Sh number correlation, indicating that the removal rate is a strong function of flow and physical properties of the system. An optimum electrolyte concentration of concentrate, sugar mass% in diluate, and applied electric potential was estimated.

Introduction

Presence of excess calcium in the post floculation and precipitation stage of clarified sugar juice creates series of nuisence [1] to sugar industries affecting product quality (listed below). Therefore, removal of it at appropriate stage would drastically reduce operation and maintainence cost and improve product quality. [1]

1. Scale formation in the evaporators

2. Improper crystallization

3. Molasses percentage may increase due to inversion of sugar in alkaline medium

4. Storage is hampered because of hygroscopic nature of these metal ions

5. Excess calcium is not hygienic as well

Application of electrodialysis (ED) is propsoed to remove the dissolved calcium ions (commonly as CaCl$_2$). Electrodialysis (ED) is a polar (cation and anion exchange) membrane based ion removal technique driven by externally applied electric potential as the main driving force. Briefly, the diluate (feed solution) containing electrolyte(s) is placed between two oppositely charged membranes through which the dissociated ions get selectively permeated. CaCl$_2$ (strong electrolyte) removal via electrolydialysis could be quite interesting to explore from industry point of view. Earlier electrodialysis (ED) was applied in sugar industry to recover speciality chemicals e.g. tartrate and malate from grape sugar [2], and in demineralisation of beet sugar syrup, juice and molasses [3,4]. Major technical obstacles arose due to poor membrane stability at higher temperatures commonly maintained to reduce solution viscosity-pumping cost and fouling due to deposition of organic molecules (sugars, proteins etc.). Difference in ionic mobility in solution and membrane causes drop in counter-ion concentration at the membrane surface, which causes concentration polarization and

adds up complexity to the existing difficulties [5-11]

In a batch recirculation ED process diluate and concentrate streams get depleted and enriched respectively with time. With increase in electrolyte concentration in the concentrate channel, back diffusion (from concentrate to diluate stream) appears affecting overall ion removal percentage. With a given diluate stream concentration, initially the current density increases with applied electric potential. Finally, it reaches a limiting value at an electric potential where no excess ions are available to transport current in solution, thus, concentration drops to zero (theoretically) at membrane surface. This is called limiting current density. Applying an electric potential above this value would result in electrolysis of water and generating H$^+$ and OH$^-$ ions. In batch recirculation mode, the diluate stream is recycled back to the ED cell to remove left over ions, therefore, gradual lowering of concentration of diluate stream occurs. Unlike continuous electrodialysis the current density keeps changing with time as is with the electrolyte concentration. Energy wastage due to water spliting is avoided by restricting current density below limiting value. Modeling of batch ED with continuous recirculation becomes more challenging as streams' electrolyte concentration changes with time. Commonly Ohm's law is applied [12-15] to evaluate current based on overall applied electric potential and resistances. But, it fails to predict several experimental current density majorly governed by ionic diffusion process, which limits the

*Corresponding author: Sujay Chattopadhyay, Polymer and Process Engineering Department, I.I.T.Roorkee, SRE Campus, UP-247 001, India, Tel: 919568189000; E-mail: sujayfpt@iitr.ernet.in; sujay1999@gmail.com

maximum magnitude of current for an applied voltage. Wen et al. [16] experimentally verified this fact and concluded that rise in ohmic resistance with lowering of diluate concentration is not significant and claimed that back emf (due to concentration polarization across the membrane) generation reduced the effective applied electric potential across the cell pair. Theoretical estimate of back emf becomes difficult due to non-availability of correct procedure. This ensured that a model probably from first principles would give us appropriate estimation of ion flux. Linearized Nernst-Plank flux equation (formulated from first principles) provided closure prediction of current density and ion flux and can quantitatively estimate drop in ion concentration. The entire batch operation was subdivided into small multiple equilibrium steps involved in irreversible thermodynamics [17].

Kabay et al. [18] carried out batch removal of bivalent Ca^{2+} and Mg^{2+} ions under constant applied DC potentials (3 V, 5 V and 10 V) and flowrates (0.6, 1.2 and 1.8 L.min^{-1}) and compared energy consumptions. Although time of operation is reduced with applied electric potential but energy consumption has increased. While, flow rate variation did not show much effect on ion removal rate. Several studies [2,18] are reported on Ca^{2+} ion removal using batch recirculation electrodialysis but, role of concentrate concentration on ion removal rate was not emphasized adequately. Herein, we tried to explore few querries: (i) Is there any optimum concentrate concentration for a given diluate composition? (ii) Is there any role of non electrolyte and its concentration (density and viscosity) on ion removal rate and energy consumption? (iii) Can we theoretically model the ion transport and estimate the transport properties? (iv) Is there a generalization possible? To the best of our knowledge, answers to these questions lacks clarity and quantitativeness. Answers to these issues might give a better insight to ion transport mechanism and optimize concentrate compartment.
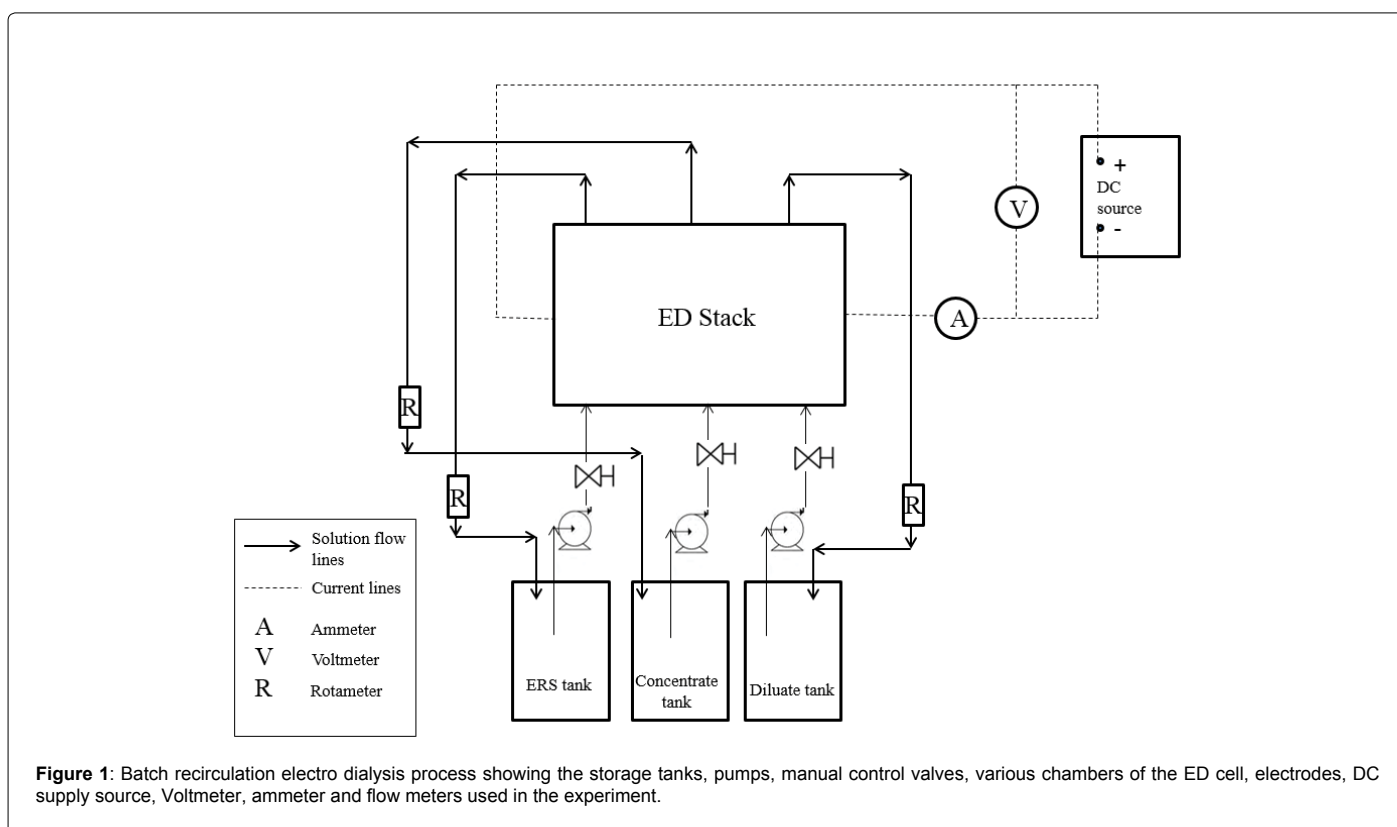
In cane based sugar industry concentration of sugar in the juice after clarification step (after lime treatment and color removal) commonly reaches ~5% (mass basis). CaCl₂ concentration is chosen based on free lime concentration left in clarified juice and the stream entering into evaporator. Role of non electrolyte (sugar), concentrate concentration and CaCl₂ viscosity on removal were investigated. A model accounting all experimental observations was used to estimate transport properties involved.

Materials and Methods

Equipment

Electro dialysis setup: The experimental setup layout used for Electrodialysis (ED) application is shown in Figure 1. The ED cell assembly was tailor made in the laboratory and graphite sheets were used as electrodes (0.08×0.04 m²). An electric DC potential was applied across the cell stack (consisted of two cell pairs containing a concentrate and a diluate channel each.) through a built-in DC source. Voltage and current between two electrodes were continually monitored through a built-in digital voltmeter and ammeter respectively. Cross linked Styrene-divinyl benzene copolymer membranes were obtained from Permionics Ltd. India and used as ion exchange membranes. The properties of the membranes were listed in Table 1. Experiments were performed at a constant applied electric potential of 4 V and a fixed flow-rate for all streams.

Power Supply: The power supply was provided through a voltage stabilizer of 110/220 V AC with 50-80 Hz frequency. The same gave an output voltage 0-20 V DC and had an ammeter that can measure currents from 0-200 mA. Three centrifugal pumps were inbuilt with the system for pumping the solution.

Figure 1: Batch recirculation electro dialysis process showing the storage tanks, pumps, manual control valves, various chambers of the ED cell, electrodes, DC supply source, Voltmeter, ammeter and flow meters used in the experiment.

Conductivity Measurement: Solution conductivity was noted at regular interval through an off line Conductivity and TDS meter CM183 from Elico India.

ED Cell Compartments and Solutions Used: 1000 ml solutions of each stream (concentrate, diluate and Electrode rinsing solution (ERS)) were taken in three tanks (Figure 1) respectively. Each solution tank was connected with its respective flow points of the ED unit through flexi tubing. Solutions were circulated at a constant rate by three centrifugal pumps and the solution flow rates were measured using rotameters connected to each stream. The detailed concentrations of different electrolyte streams were reported in Table 2. Concentrate and diluate solutions were always prepared using deionized water (conductivity <10.0 μS). Electrodialysis experiments were carried out in three sets. (i) DSC1-DSC6 (diluate stream having 25 mol.m⁻³ CaCl₂ and 5 mass% sugar and six different concentrate streams having CaCl₂ concentrations varying as 5, 10, 20, 25, 30, and 40 mol.m⁻³), (ii) C1-C6 (diluate stream having 25 mol.m⁻³ CaCl₂ and six different concentrate streams with CaCl₂ concentrations as 5, 10, 20, 25, 30, and 40 mol.m⁻³) and (iii) S1-S4 (4 different diluate streams with 25 mol.m⁻³ CaCl₂ with amount of sugar varying from 5-20 mass% and concentrate stream having concentration of 25 mol.m⁻³ CaCl₂). For convenience DSC4 is renamed as S1 (5 mass% sugar) as both the experiments are identical and other values of sugar concentration are defined as S2 (10 mass% sugar), S3 (15 mass% sugar) and S4 (20 mass% sugar). Detailed information was reported in Table 2. Aqueous solution of NaCl (50 mol.m⁻³) was used as ERS in all experiments (Table 2). The detailed specifications of ED unit are indicated in Table 3.

Limiting current density (LCD): LCD of the ED cell was estimated using the method reported in the literature [5,15] by plotting cell resistance (V/I) vs. inverse of current (1/I).

Viscosity measurement: Ubbelhood viscometer was fitted in a constant temperature bath to measure solution viscosity at a desired temperature (±1°C). Sugar concentration was varied between 0-20 mass%, while CaCl₂ concentration was varied between 0-50 mol.m⁻³ to estimate the solution viscosity.

Modelling of ion transport: Current density and LCD (limiting current density) of an ED cell is a function of series of parameters e.g. flow (cell geometry, flow dynamics, spacer orientation, solution density and viscosity) and physical (ion concentration, transport number and diffusivity) parameters for a given set of membrane pairs. Precise estimation of these parameters and application of Nernst-Plank equation (assuming zero ion concentration on the membrane surface) would give a theoretical estimate of LCD which can be determined experimentally from plot of V/I vs. 1/I [5,6].

Determination of bulk concentration of diluate compartment

The ED process was carried out well below LCD all through.

The concentration of ion can be obtained from unsteady mass balance across diluate, concentrate, and electrode compartments. The unsteady state mass balance equation was formulated based on the assumptions already mentioned in the literature [12].

The mass balance equations for diluate and concentrate compartments in the ED cell are written as [12,13]

$$NV_C^{dil}\frac{dC^{dil}}{dt} = Q^{dil}\left(C_T^{dil} - C^{dil}\right) - \frac{N\eta i A_m}{ZF} + \frac{NA_m D_{AEM}\left(C_{AEM}^{conc} - C_{AEM}^{dil}\right)}{l_{AEM}} + \frac{NA_m D_{CEM}\left(C_{CEM}^{conc} - C_{CEM}^{dil}\right)}{l_{CEM}} \quad (1)$$

$$NV_C^{conc}\frac{dC^{conc}}{dt} = Q^{conc}\left(C_T^{conc} - C^{conc}\right) - \frac{N\eta i A_m}{ZF} + \frac{NA_m D_{AEM}\left(C_{AEM}^{conc} - C_{AEM}^{dil}\right)}{l_{AEM}} + \frac{NA_m D_{CEM}\left(C_{CEM}^{conc} - C_{CEM}^{dil}\right)}{l_{CEM}} \quad (2)$$

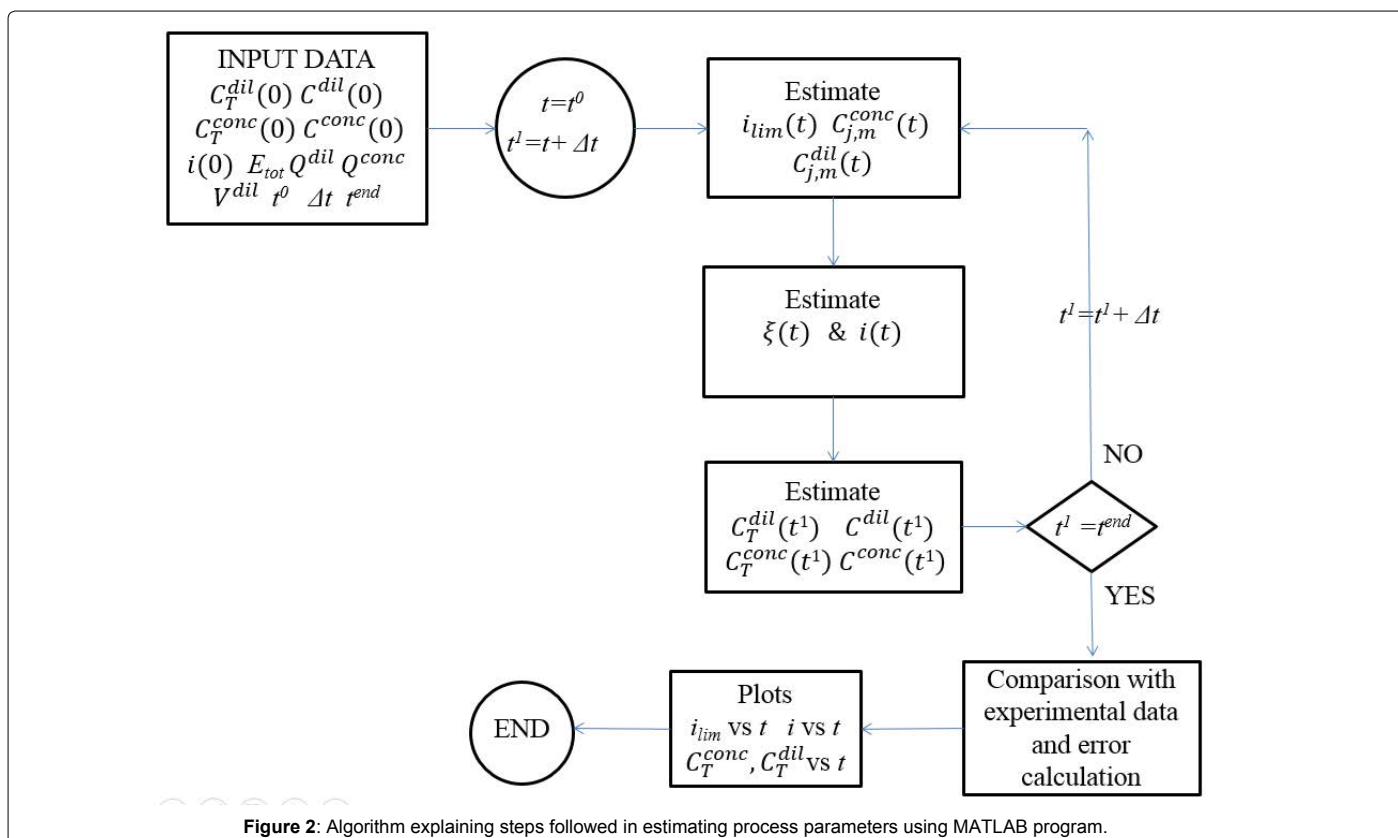Where, V_C^{dil}, $V_C^c onc$ are the volumes of diluate and concentrate

Figure 2: Algorithm explaining steps followed in estimating process parameters using MATLAB program.

Physical Parameters	Cation exchange Membrane	Anion exchange Membrane
Transport number	0.91	0.9
Experimental Resistance (ohm cm^{-2})	2.0-3.5	-----
Max. pressure allowed (kgcm^{-2})	3.0	3.0
Thickness (mm)	0.11 to 0.15	0.09 to 0.11
Max Temperature (°C)	60	60

Table 1: Membrane parameters as obtained from Permionics India Ltd.

Expt. no.	Concentrate	Concentrate 10^6(m³.s^{-1})	Diluate	Diluate 10^6(m³.s^{-1})	ERS	10^6(m³.s^{-1})	Voltage applied (V)	Time (min)
	SC		Concentrate concentration varied			5% sugar in diluate		
DSC1	Aqueous 5 mol.m^{-3} CaCl₂	8.43	25 mol.m^{-3} CaCl₂ in 5% sugar solution	8.78	Aqueous 50 mol.m^{-3} NaCl solution	9.15	4	150
DSC2	Aqueous 10 mol.m^{-3} CaCl₂ solution	8.43	25 mol.m^{-3} CaCl₂ in 5% sugar solution	8.78	Aqueous 50 mol.m^{-3} NaCl solution	9.15	4	150
DSC3	Aqueous 20 mol.m^{-3} CaCl₂ solution	8.43	25 mol.m^{-3} CaCl₂ in 5% sugar solution	8.78	Aqueous 50 mol.m^{-3} NaCl solution	9.15	4	150
DSC4	Aqueous 25 mol.m^{-3} CaCl₂ solution	8.43	25 mol.m^{-3} CaCl₂ in 5% sugar solution	8.78	Aqueous 50 mol.m^{-3} NaCl solution	9.15	4	150
DSC5	Aqueous 30 mol.m^{-3} CaCl₂ solution	8.43	25 mol.m^{-3} CaCl₂ in 5% sugar solution	8.78	Aqueous 50 mol.m^{-3} NaCl solution	9.15	4	150
DSC6	Aqueous 40 mol.m^{-3} CaCl₂ solution	8.43	25 mol.m^{-3} CaCl₂ in 5% sugar solution	8.78	Aqueous 50 mol.m^{-3} NaCl solution	9.15	4	150
	C		Concentrate concentration varied			No sugar in diluate		
C1	Aqueous 5 mol.m^{-3} CaCl₂	8.43	Aqueous 25 mol.m^{-3} CaCl₂ solution	8.78	Aqueous 50 mol.m^{-3} NaCl solution	9.15	4	150
C2	Aqueous 10 mol.m^{-3} CaCl₂ solution	8.43	Aqueous 25 mol.m^{-3} CaCl₂ solution	8.78	Aqueous 50 mol.m^{-3} NaCl solution	9.15	4	150
C3	Aqueous 20 mol.m^{-3} CaCl₂ solution	8.43	Aqueous 25 mol.m^{-3} CaCl₂ solution	8.78	Aqueous 50 mol.m^{-3} NaCl solution	9.15	4	150
C4	Aqueous 25 mol.m^{-3} CaCl₂ solution	8.43	Aqueous 25 mol.m^{-3} CaCl₂ solution	8.78	Aqueous 50 mol.m^{-3} NaCl solution	9.15	4	150
C5	Aqueous 30 mol.m^{-3} CaCl₂ solution	8.43	Aqueous 25 mol.m^{-3} CaCl₂ solution	8.78	Aqueous 50 mol.m^{-3} NaCl solution	9.15	4	150
C6	Aqueous 40 mol.m^{-3} CaCl₂ solution	8.43	Aqueous 25 mol.m^{-3} CaCl₂ solution	8.78	Aqueous 50 mol.m^{-3} NaCl solution	9.15	4	150
	S		Mass% of sugar varied in diluate					
S1	Aqueous 25 mol.m^{-3} CaCl₂ solution	8.43	25 mol.m^{-3} CaCl₂ in 5% sugar solution	8.78	Aqueous 50 mol.m^{-3} NaCl solution	9.15	2	150
S2	Aqueous 25 mol.m^{-3} CaCl₂ solution	8.43	25 mol.m^{-3} CaCl₂ in10% sugar solution	8.78	Aqueous 50 mol.m^{-3} NaCl solution	9.15	4	150
S3	Aqueous 25 mol.m^{-3} CaCl₂ solution	8.43	25 mol.m^{-3} CaCl₂ in 15% sugar solution	8.78	Aqueous 50 mol.m^{-3} NaCl solution	9.15	6	150
S4	Aqueous 25 mol.m^{-3} CaCl₂ solution	8.43	25 mol.m^{-3} CaCl₂ in 20% sugar solution	8.78	Aqueous 50 mol.m^{-3} NaCl solution	9.15	8	150

Table 2: Different process variables chosen during ED experimentation.

Parameter	Value	Reference
Temperature, T	308 K	This work
Transport number of cation in the solution,2+,	0.4387	This work [5]
Transport number of anion in the solution,	0.5613	This work [5]
Diffusivity of Ca^{2+} ions in solution at 20˚C	7.92×10^{-10} m².s^{-1}	This work [25,26]
Diffusivity of Cl$^-$ ions in solution at 20˚C,	17.7×10^{-10} m².s^{-1}	[5]
Diffusivity of CaCl2 through AEM	1.8×10^{-11} m².s^{-1}	[30]
Diffusivity of CaCl2 through CEM	1.8×10^{-11} m².s^{-1}	[30]
Distance between adjacent membranes	4.7×10^{-3} m	This work
Area of the membrane, Am	32×10^{-4} m²	This work
Charge on the Calcium ion,2+	+2	This work
Current efficiency,	0.81	This work
Sh number empirical equation constant, a	0.0583 ± 0.0045	This work
Sh number empirical equation constant, b	0.63	This work [24]
Sh number empirical equation constant, c	0.33	This work [24]
Sh number empirical equation constant, d	-0.131	This work

Table 3: Values of different physical parameters used in the model.

compartments (m³) respectively, N is number of cell pairs, t is time (s), $C_T^{d}il$ and C_T^{conc} represents diluate concentrations, leaving diluate feed tank and leaving diluate cell compartment (mol.m⁻³) respectively, C_T^{conc} and $Q^{d}il$ represents diluate concentrations, leaving concentrate feed tank and leaving concentrate cell compartment (mol.m⁻³) respectively, $Q^{d}il$ and , $Q^{c}onc$ are the diluate and concentrate streams volumetric flow rate (m³.s⁻¹), η is the current efficiency, t is the current density (A.m⁻²), η is the effective membrane area (m²).

η can be estimated from the following equation [12,13]:

$$\eta = t_{+,CEM} + t_{-,AEM} - 1 \tag{3}$$

Where, $t_{-,AEM}$ is the transport-number of cations in cation exchange membranes and $t_{-,AEM}$ is the transport-number of anions in anion exchange membrane.

Similarly, unsteady state mass balance around feed tank can be written as

$$\frac{(d(V_T^c onc C_T^c onc))}{dt} = Q^c onc(C^c onc - C_T^c onc) \tag{4}$$

$$\frac{(d(V_T^c onc C_T^c onc))}{dt} = Q^c onc(C^c onc - C_T^c onc) \tag{5}$$

Where V_T^{conc} and V_T^{conc} are volumes of concentrate and diluate feed tanks (m³) respectively. During electrodialysis water transport occurs across the membranes due to electro-osmosis and osmosis [13]. In the present work volume change (due to water transport) is ignored as there was no major net volume change observed (concentrate and diluate compartments) experimentally.

Determination of the current density

Overall flux equation : The current density was estimated using following assumptions (usually valid for all practical situations) [13]. The solution between the two membranes was assumed, thoroughly mixed to ensure uniform concentration throughout. Stationary membrane surfaces leads to the formation of static boundary layer whose thickness is mainly governed by solution viscosity and existing turbulence. Fluid flow alone can determine the boundary layer thickness [5]. Ion transport due to convection was ignored [19] because the direction of ion transport was perpendicular to the direction of the flow. Trans-membrane pressure was assumed to be zero. Stable boundary layers are formed along the concentrate and diluate compartments of the membrane due to difference in viscosity of feed and concentrate solution. The current density can be estimated from mass balance equation either for cations through CEM or anions through AEM, assuming overall (sum) transport numbers to be unity. The flux of ions passing through the membrane can be expressed by generalized Nernst Plank equation as [5]

$$N_j = -D_j \frac{\partial C_j}{\partial x} - \frac{z_j C_j F D_j}{RT} \frac{\partial \psi}{\partial x} \tag{6}$$

Where, x is the distance measured from boundary layer in contact with the diluate channel towards the membrane, C_j is the diffusivity of ion j (either cation or anion) (m².s⁻¹), 'C_j is the concentration of ion j (mol.m⁻³), 'R' is the universal gas constant (8.314 J.mol⁻¹.K⁻¹), 'T' is the temperature (K), 'z_j' is the charge of diffusing species j, and $N_{j,}$ is the electric potential gradient (V.m⁻¹) and F is the faradays constant (Columb.geqv⁻¹).

The total molar flux of ion 'j' through the ion exchange membrane, $N_{j,m}$ can be related to the current density, i as

$$N_{j,m} = \frac{t_{j,m} i}{z_j F} \tag{7}$$

The subscript m denotes either AEM or CEM, Z_j is the transport number of ion 'j' in the membrane, i is current per unit area of membrane or current density (A.m⁻²) and Z_j is the charge of the ion.

At steady state $N_{j,m}$ and $N_{j,m}$ are equal, i.e.:

$$\frac{t_{j,m} i}{Z_j F} = -D_j \frac{\partial C_j}{\partial x} - \frac{Z_j C_j F D_j}{RT} \frac{\partial \psi}{\partial x} \tag{8}$$

Assuming that a linear profile of the concentration distribution exists along the boundary layer, the linearized Nernst-Planck equation could be used instead of Eq. (8). Expression for the linearized Nernst-Planck equation when applied in the diluate chamber is [5]:

$$\frac{t_{j,m} i}{z_j F} = \frac{D_j \left(C_{(j,b)}^{dil} - C_{j,m}^{dil} \right)}{\delta} - \frac{z_j D_j F \xi C_{j,m}^{dil}}{RT} \tag{9}$$

Where, δ is the boundary layer thickness (m), $C_{(j,b)}^{d}il$ and $C_{(j,m)}^{d}il$ are concentrations of ions in bulk and at the membrane surface respectively of the diluate compartment, while ξ is the electric potential gradient (V.m⁻¹) and is expressed as

$$\xi = \frac{\psi}{\delta} \tag{10}$$

where, δ is the boundary layer thickness.

In Eq. (9) the first part, i.e., $\frac{D_j \left(C_{j,b}^{dil} - C_{j,m}^{dil} \right)}{\delta}$ denotes contribution due to molecular diffusion while the second part i.e., $\frac{z_j D_j F \xi C_{j,m}^{dil}}{RT}$ reflects the effect of voltage on ion-transfer through the membrane.

Boundary layer thickness, δ estimation: δ is estimated using film theory (Eq. (11)) [5,20] and salt mass-transfer coefficient. Salt mass-transfer coefficient is usually determined based on salt diffusivity and suitable mass-transfer correlation, which in-turn is dependent on flow profile and physical properties of the fluids, cell geometry, surface morphology of membranes used in ED cell [5,6,19,21,22].

$$\delta = \frac{D_j}{k} \tag{11}$$

Where, k and k are diffusivity and mass transfer coefficient of diffusing species in solution. Each of these parameters were separately estimated using standard correlations. The mass transfer coefficient was obtained from Sherwood number. [5,19,20] as:

$$Sh = \frac{k.l}{D_j} \tag{12}$$

Where, l is the characteristic length (m). Sherwood number Sh, is expressed as a function of Reynolds number, Re and Schmidt number, Sc [5,20]. The empirical expression of Sherwood number is based on cell geometry and spacer configuration chosen for the present cell is indicated below [20-24]

$$Sh = a. Re^b. Sc^c. \left(\frac{\ddot{E}_{Dil}}{\ddot{E}_{Conc}} \right)^d \tag{13}$$

Where, Sc (Schmidt's number, $\mu/\rho D_j$ is estimated from physical properties (viscosity and density) of the medium while Reynolds number, $\left(\frac{\rho vl}{\mu} \right)$ indicates flow characteristics of the medium [20] and $\left(\frac{\Lambda_{Dil}}{\Lambda_{conc}} \right)$ represent the conductivity ratios of diluate and concentrate, while 'a' 'b' 'c' 'd' are the empirical constants.

Ionic diffusivity is a strong function of hydrodynamic diameter of ions. Assuming infinite dilution ionic diffusivity is estimated using the Nernst-Haskel equation (Eq. 14) [25] as:

$$D^\circ = \frac{RT}{F^2} \frac{\left[(1/Z+) + (1/Z-) \right]}{\left[(1/\lambda_+) + (1/\lambda_{-1}) \right]} \qquad (14)$$

Where z_+ and z_- denote charges of cation and anion respectively while λ_+ and λ_- denotes limiting ionic conductance in the solvent. Other parameters bearing meaning and units are as reported in the nomenclature.

In general diffusivity of ions from electrolytes e.g. NaCl, CaCl$_2$, LiCl in water are closely related to changes in solution viscosity at constant temperature. Therefore, necessary correction of diffusivity on viscosity is essential. Li et al. [26] experimentally verified that diffusivity of ions in an electrolyte solution is inversely proportional to the solution viscosity.

$$\frac{D}{D^\circ} = \frac{\mu^\circ}{\mu} \qquad (15)$$

Therefore, the estimated diffusivities were corrected due to solution viscosity.

Estimation of Membrane Surface Concentration: The membrane surface concentration of ions is dependent on current density under an applied voltage. As long as the ED operation is executed below limiting current (surface concentration would become zero at limiting current), the surface concentration on either side can be estimated from bulk concentration measurement (diluate/concentrate), current density and limiting current density using Eqs. (16) and (17) [13,27].

$$C_{(j,m)}^c onc = C_j^c onc(1 + i / i_{j,lim}) \qquad (16)$$

$$C_{j,m}^{dil} = C_j^{dil} (1 - i / i_{j,lim}) \qquad (17)$$

Where, $C_{j,m}^{conc}$ and C_j^{conc} are the concentrations of ion j, at the membrane surface and in bulk of the concentrate compartment respectively in the ED cell. $C_{j,m}^{dil}$ and C_j^{dil} are the concentrations of ion j, at the membrane surface and in the bulk of the diluate side respectively in the ED cell.

Estimation of current density and limiting current density (i **and** $i_{j,lim}$ **):** LCD (of a single electrolyte) is estimated from linearized Nernst Planck equation [6,8]:

$$i_{j,lim} = \frac{C_{j,b}^{dil} D_j Z_j F}{\delta (t_{j,m} - t_j)} \qquad (18)$$

Where, $t_{j,m}$ and t_j are transport numbers of ion j in membrane and electrolyte solution respectively.

Considering ion flux in the diluate side of the IEM, Eq. (17) is used to calculate concentration of ion j, at the membrane surface of diluate side $C_{j,m}^{dil}$

The current density can be expressed by Eq. (17) after substitution of Eqs. (17) and (18) in Eq. (8).

$$i = \frac{C_{j,b}^{dil} D_j Z_j \xi \frac{F}{RT}}{\frac{t_{j,m} - t_j}{Z_j F} + \frac{\xi \delta (t_{j,m} - t_j)}{RT} - \frac{t_{j,m} Z_j}{F}} \qquad (19)$$

Where ξ, the electric potential gradient can be estimated from Nernst equation given below [12,13]

$$\xi = -(2t_{j,m} - 1) \frac{RT}{\delta F} ln \left(\frac{\gamma_b^{dil} C_{j,b}^{dil}}{\gamma_m^{dil} C_{j,m}^{dil}} \right) \qquad (20)$$

Where γ_m^{dil} and γ_b^{dil} are the mean ionic activity coefficients corresponding to the ions at the wall of IEM and in the bulk of solution respectively within the diluate channel and they are estimated using Debye–Huckel limiting law.

Numerical Estimation of Parameters

The sequence of steps followed in the model to estimate current density and concentration change is described in the flow chart (Figure 2). The differential equations (Eqs. (1), (2), (4) and (5)) were integrated using Euler method using 1 second step size interval. Initial process conditions were obtained from literature. Few crucial parameters and their estimation techniques which were not taken up earlier are presented below.

Experimental current density and concentration of Ca^{2+} ions

The current flowing through the electrolyte solution of the ED cell under an applied voltage was recorded in ammeter. Ca^{2+} ions concentration was estimated from conductivity measurement and using standard calibration chart (mass concentration vs. conductance).

Estimation of mass transfer coefficients

Mass transfer correlations for the electro dialysis process based on the cell geometry were reported earlier by several authors [15,24]. They expressed Sherwood number (Sh) as a power function of Reynolds (Re) and Schmidt number (Sc) determined from their experimentation. In this report we have developed a suitable mass transfer correlation using the LCD and current density expressions that suits all of our experimental results.

LCD was estimated experimentally for the case where both concentrate and diluate concentrations were 25 mol.m^{-3} of CaCl$_2$ in water (Figure 3). Using this LCD value and Eqs. (11), (12) and (18) along with physical properties of the electrolytes reported in Table 3, the mass transfer coefficient was estimated. Which was subsequently
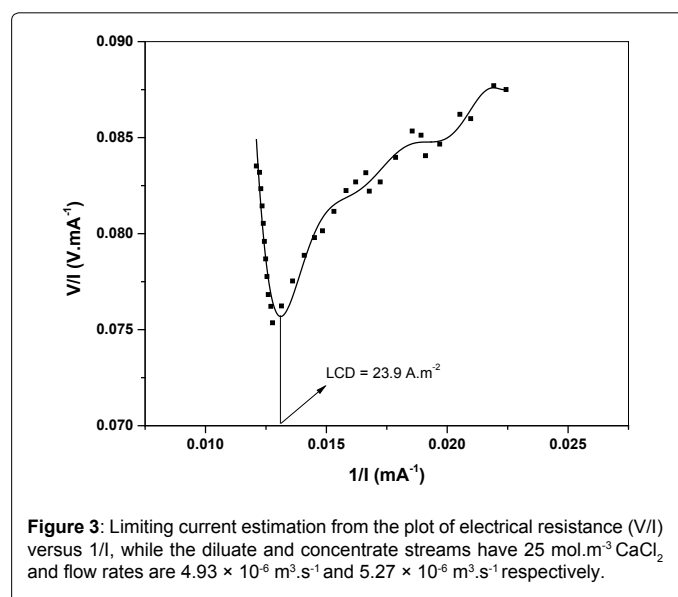

Figure 3: Limiting current estimation from the plot of electrical resistance (V/I) versus 1/I, while the diluate and concentrate streams have 25 mol.m^{-3} CaCl$_2$ and flow rates are 4.93 × 10^{-6} m^3.s^{-1} and 5.27 × 10^{-6} m^3.s^{-1} respectively.

used to evaluate Sherwood number as a function of system flow parameters e.g. Reynolds number, Schmidt number and dimensionless ratio of conductivities Eq. (13). It was found that $Sh.Sc^{-0.33}$ was a linear function of $Re^{0.63}$, where $Sh.Sc^{-0.33} = 0.0583 . Re^{0.63}$.

The constant 0.0583 is a product of parameters a and $\left(\frac{\Lambda_{Dil}}{\Lambda_{Conc}}\right)^d$. For the set with same CaCl₂ concentration in concentrate and diluate streams, the ratio of conductivity values is close to unity $\left(\frac{\Lambda_{Dil}}{\Lambda_{Conc}}\right) \sim 1.0$. This makes the factor $a = 0.0583$. The factor $a.\left(\frac{\Lambda_{Dil}}{\Lambda_{Conc}}\right)^d$ was optimized to fit each experimental data point (concentration and current density with time). From each of this optimum value, d was obtained knowing $\left(\frac{\Lambda_{Dil}}{\Lambda_{Conc}}\right)$ for any set and is found out to be -0.131. The Sherwood number correlation suitable for the ED cell flow channel geometry was obtained as

$$Sh = (0.0583 \pm 0.0045).Re^{0.63}.Sc^{0.33}.\left(\frac{\Lambda_{Dil}}{\Lambda_{Conc}}\right)^{-0.131} \qquad (21)$$

The proposed equation (Eq. 21) has been validated and reported in Appendix.

Determination of transport number of ion in solution

Transport number t_j of ion j is the fraction of total current carried by the ion type which is a function of diffusion coefficient and ionic mobility of hydrated species. Difference in hydration ability influences size, diffusivity and mobility of the ion. Thus, ions do not transport current equally in solution. The transport number was estimated from the following equation [5]:

$$t_j = \frac{|z_j| D_j C_j}{\sum_{j=1}^{n} |z_j| D_j C_j} \qquad (22)$$

For a binary-ion salt solution, $n = 2$, $j = 1$ for cation and $j = 2$ for anion and transport number is measured.

Determination of current

Initial current density estimation is essential to obtain salt concentration at membrane surface, and to start numerical integration, which may be evaluated either experimentally or from the applied electric potential and solution resistances using Ohms law. The applied electric potential may be expressed as

$$E_{tot} - E_{el} = R_{tot}.I \qquad (23)$$

Where, E_{el} is the electric potential drop near the electrodes, R_{tot} is the overall resistance (ohm) of the ED cell and I is the current (A). The overall resistance is the sum of individual values:

$$R_{tot} = R_{conc} + R_{dil} + R_{ERS} + R_{mem} \qquad (24)$$

Where, resistance of ERS, concentrate, and diluate channels were estimated either directly from conductivity measurement from extended Kohlrausch-equation [13,28]. The conductivity and the resistance are related as

$$Resistance = \frac{1}{\Lambda} \frac{L}{A_m} \qquad (25)$$

Where, Λ is the conductivity of solution (S.m⁻¹), L is the gap between membranes or the compartment thickness (m), A_m is the effective membrane area (m²).

Determination of the γ_m^{dil} and γ_b^{dil}

γ_b^{dil} and γ_b^{dil} are the mean ionic activity coefficients of salt at

membrane and in bulk respectively in the diluate. These were estimated using Debye-Huckel limiting law [28].

$$\log \gamma_{\pm} = \frac{-0.511|z_+ \cdot z_-|I_s^{1/2}}{1 + I_s^{1/2}} \qquad (26)$$

Where $\gamma_{\pm}$ is the mean ionic activity of a salt in an electrolyte solution and I_s is the ionic strength defined as,

$$I = 0.5\sum m_j z_j^2 \qquad (27)$$

Where m_j is molality (mol/kg solution) of the ion 'j' having charge E_{sp}.

CaCl₂ solution (with 5% sugar) densities were estimated experimentally and these data were linearly regressed ($R^2 = 0.984$) and used whenever required (Figure 4).

Determination of specific energy consumption

The specific energy consumption, E_{sp} (kWh.kg⁻¹) was estimated from the following equation

$$E_{sp} = \frac{\int_{t_1}^{t_2} \varepsilon A_m i(t) dt}{M_{CaCl_2} \Delta n_{CaCl_2}(t)} \qquad (28)$$

Where, ε is the applied electric potential in volt, M_{CaCl_2} is the area of the membrane in m², $i(t)$ is the current density (A.m⁻²) as a function of time, M_{CaCl_2} is the molecular mass of CaCl₂ (=111.02 g.mol⁻¹), and $\Delta n_{cacl_2}(t)$ is the number of moles of CaCl₂ removed from the feed solution at various time interval.

Results and Discussions

Role of Sugar (mass%) and CaCl₂ concentration on solution viscosity and influence of temperature

Sugar solution viscosity measurement at constant temperature shows nonlinear (Figure 5) rise with sugar (5 to 20 mass%). Viscosity values were found to be between 0.72 - 1.5 mPa.s with increase in sugar mass%. These values were very much comparable with the literature reported data [29]. Solution viscosity does not show appreciable change with CaCl₂ concentration (0-50 mol.m⁻³) (Figure 6). Viscosity measurement of CaCl₂ solution at 20, 25, 32, 37, 42°C show lowering
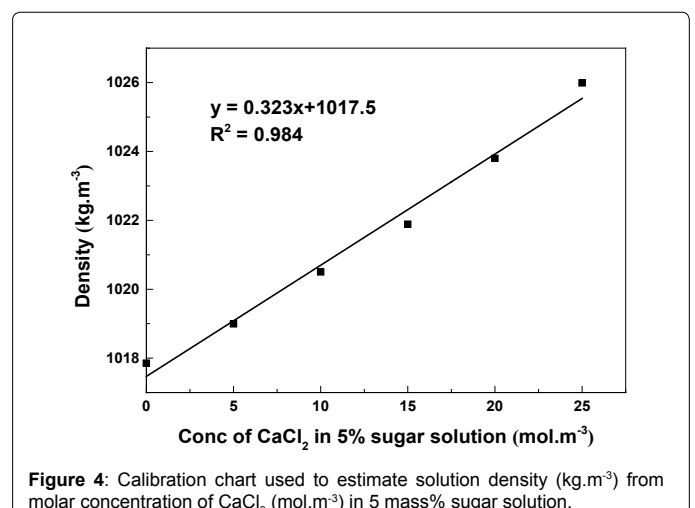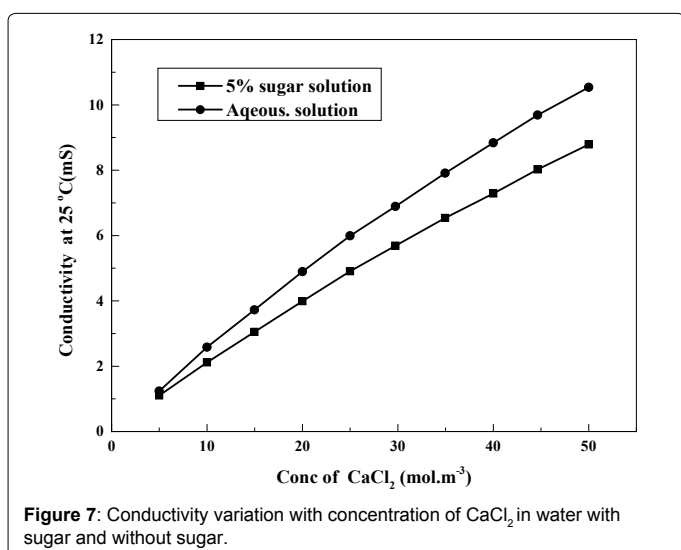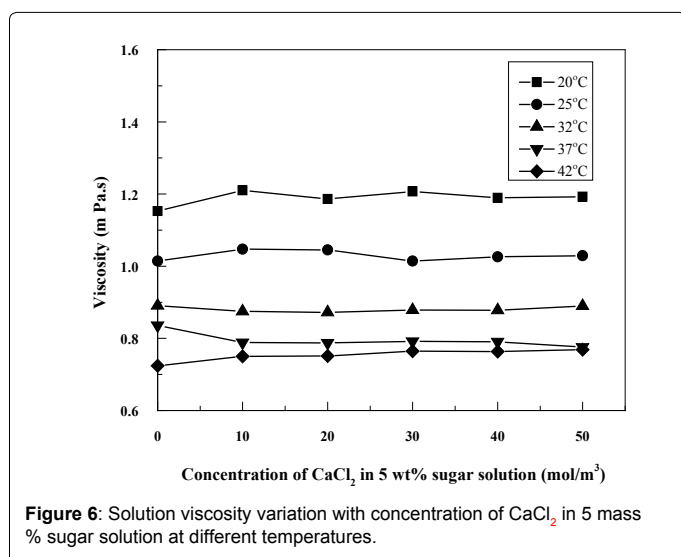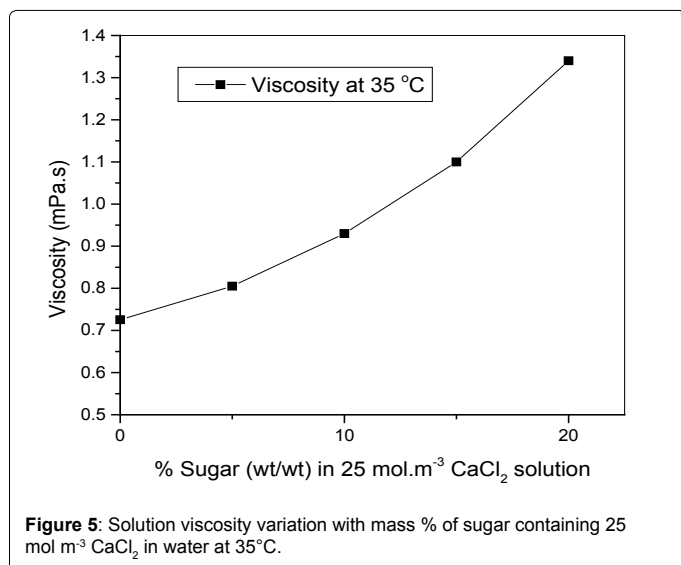

Figure 4: Calibration chart used to estimate solution density (kg.m⁻³) from molar concentration of CaCl₂ (mol.m⁻³) in 5 mass% sugar solution.

Figure 5: Solution viscosity variation with mass % of sugar containing 25 mol m^{-3} CaCl$_2$ in water at 35°C.

Figure 6: Solution viscosity variation with concentration of CaCl$_2$ in 5 mass % sugar solution at different temperatures.

Figure 7: Conductivity variation with concentration of CaCl$_2$ in water with sugar and without sugar.

between 1.18 to 0.6 mPa.s. Almost ~37% lowering in viscosity was recorded (Figure 6).

Effect of Sugar and CaCl$_2$ concentration on electrical conductivity

Figure 7 shows plot of electrical conductivity with CaCl$_2$ concentration, estimated in presence and absence of sugar. Solution conductivity increases almost linearly with rise in CaCl$_2$ concentration (5 to 50 mol.m^{-3}). CaCl$_2$, a strong electrolyte, dissociates completely in solution and increase number of ions per unit volume available for ionic conductance. Addition of sugar dampens the ion conductivity values. This may be due to sugar, a water soluble non-electrolyte, doesn't dissociate and change the number of ions responsible for current carriage, therefore, presence of inert sugar molecules causes increase in crowding in solution.

Experimental results and model prediction

The LCD measurement by plotting V/I vs. 1/I (Figure 3) (diluate and concentrate concentrations are 25 mol.m^{-3} CaCl$_2$) shows a minima at 0.013 mA^{-1} which corresponds to the applied electric potential ~6 V. All experiments were categorically performed at 4 V, hoping current density to remain always below limiting value because, initial concentration of CaCl$_2$ in the diluate stream was kept unchanged for all experiments.

Current density and concentrate concentration variation were noted at regular interval for all the experiments and reported in Figures 8-10. With progress of electrodialysis current density gets lowered (Figure 8) while, concentrate CaCl$_2$ concentration increased (Figure 9). Lowering of the initial CaCl$_2$ concentration in concentrate stream (C6 to C1, Figure 8) for the same diluate stream current density dropped. Similar trend was noted with increase in sugar mass% in the diluate channel (DSC6 to DSC1, Figure 8), but overall current density values were lower than the corresponding non-sugar cases (Figures 8 and 10) shows current density is a strong function of sugar concentration i.e. with increase in sugar mass% (S1, 5% to S4, 20%) the current density drops.
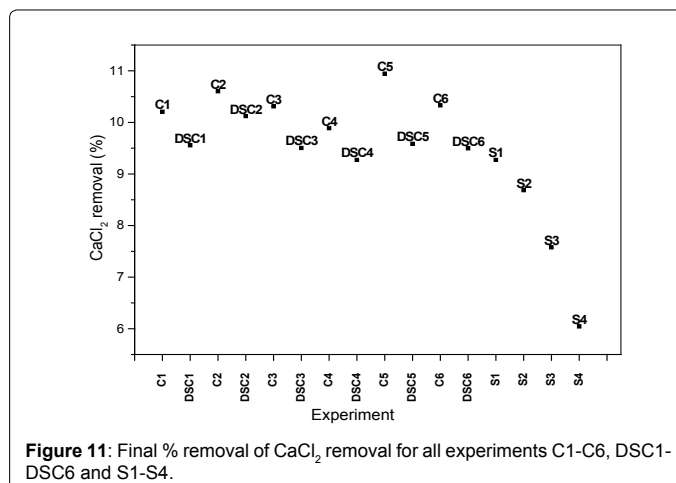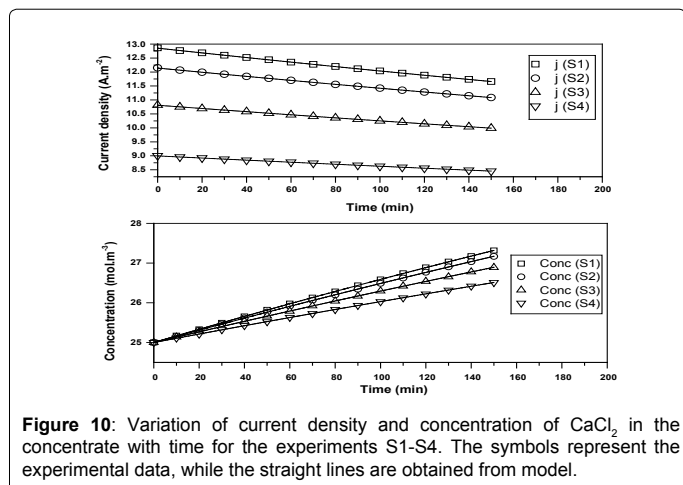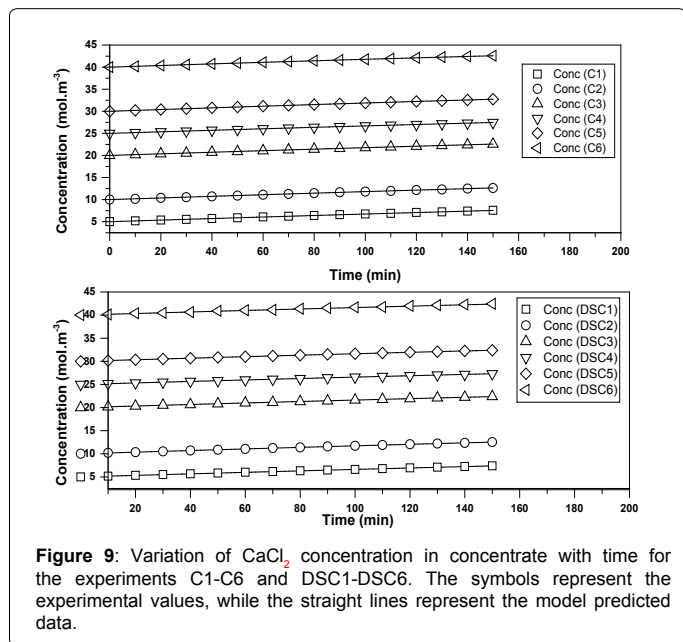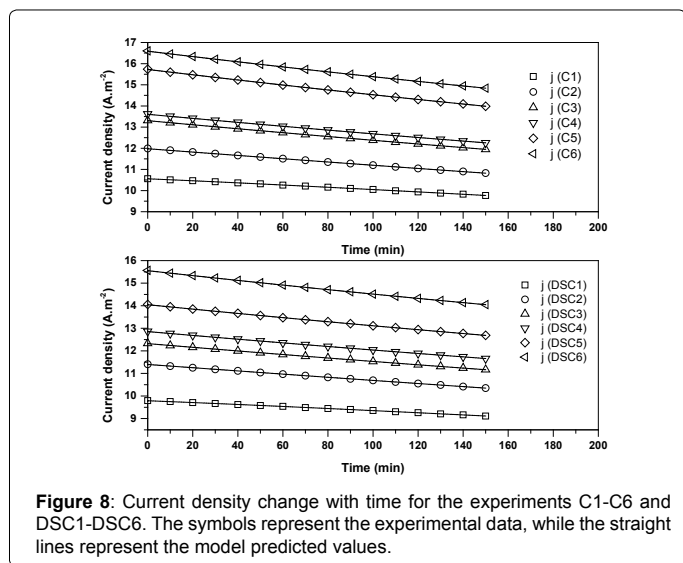
The ion removal percentage estimated from the initial and final CaCl$_2$ concentration of the diluate channel (Figure 11) doesn't show any trend with concentrate concentration. Experiments C5 and DSC2 showed higher ion removal among their corresponding sets C1-C6 and DSC1-DSC6 respectively (Figure 11). This possibly hints at presence of a series of complex reaction taking place in ion transport.

Presence of sugar in the diluate (DSC1-DSC6) stream reduced ion removal rate compared to corresponding non-sugar cases (C1-C6). This may be attributed to tremendous defiance experienced by hydrated calcium ions in presence of inert sugar molecules.

Eqs. (1), (4), (2) and (5) along with initial conditions (Table 3) were solved as per the reported sequence (Figure 2) using MATLAB. The solution gave us theoretical estimate of concentration. Predicted molar concentration of both concentrate and diluate stream shows nice agreement with all experimental data. This is represented by continuous line (Figures 8-10) showing an excellent agreement with the experimental data.

Effect of concentrate stream concentration

Influence of concentrate stream concentration on (i) overall current density (Figure 8), and (ii) ion removal rate (percentage) from diluate solution (Figure 11) were experimentally estimated. Figure 8

Figure 8: Current density change with time for the experiments C1-C6 and DSC1-DSC6. The symbols represent the experimental data, while the straight lines represent the model predicted values.

Figure 9: Variation of CaCl$_2$ concentration in concentrate with time for the experiments C1-C6 and DSC1-DSC6. The symbols represent the experimental values, while the straight lines represent the model predicted data.

Figure 10: Variation of current density and concentration of CaCl$_2$ in the concentrate with time for the experiments S1-S4. The symbols represent the experimental data, while the straight lines are obtained from model.

Figure 11: Final % removal of CaCl$_2$ removal for all experiments C1-C6, DSC1-DSC6 and S1-S4.

shows increase in current density with rise in initial concentration of CaCl$_2$, which decreases slowly with time. This is true for both types of diluate with sugar and without sugar. Initially high current density value is probably due to availability of dissociated Ca^{2+} and 2Cl$^-$ ions of CaCl$_2$ (a strong electrolyte). With increase in CaCl$_2$ concentration, more such dissociated species appear per unit volume which reduces overall solution resistance and increases current density under a given electric potential. A slow drop in current value appeared due to gradual depletion of ions from diluate compartment. Figure 11 showing percentage removal from diluate stream didn't follow any trend probably due to involvement of several competing factors in overall ion removal. The current density values (Figure 8) don't predict the net ion removal percentage, instead overall ion removal depends on effective or net flux existing in the cell. Effective ion removal rate is due to cumulative addition of two competing processes namely: (i) An external applied electric potential and (ii) chemical potential (or diffusive transport) arising out of concentration gradient across the membrane. The applied electric potential always tries to push Ca^{2+} ions towards the appropriate electrode while, the direction of chemical potential or diffusive transport is decided by the concentration gradient across the membrane. Flux components arising out of an applied electric potential (hence forth defined as current flux), concentration gradient (diffusive flux) and overall (net) flux were estimated from model and presented in Figure 12.

The current flux increased with CaCl$_2$ concentration in the concentrate stream in the sequence C1-C6 and DSC1-DSC6. The trend is similar to the current density behavior indicated before. The diffusive component is favorable for C1 and DSC1 (values are positive), while for C2 and DSC2 it is favorable till initial 40 minutes but thereafter it becomes unfavorable. This leads to crossover of net flux and current flux lines (Figures 12a-12c). Similar crossover doesn't arise with any set, because, the diffusive component remained consistently either positive or negative for the rest of the experiment. Ion removal being a complex process gets influenced by e.g. concentrate concentration, the solution viscosity, conductivity, concentration of non-electrolyte (taken up in the following section) even if the applied electric potential, flow rate and cell geometry were kept unchanged. Concentrate Ca^{2+} concentration being lower than diluate stream the diffusive part becomes favorable for initial 40 minutes and thereafter it gets reversed causing cross over.
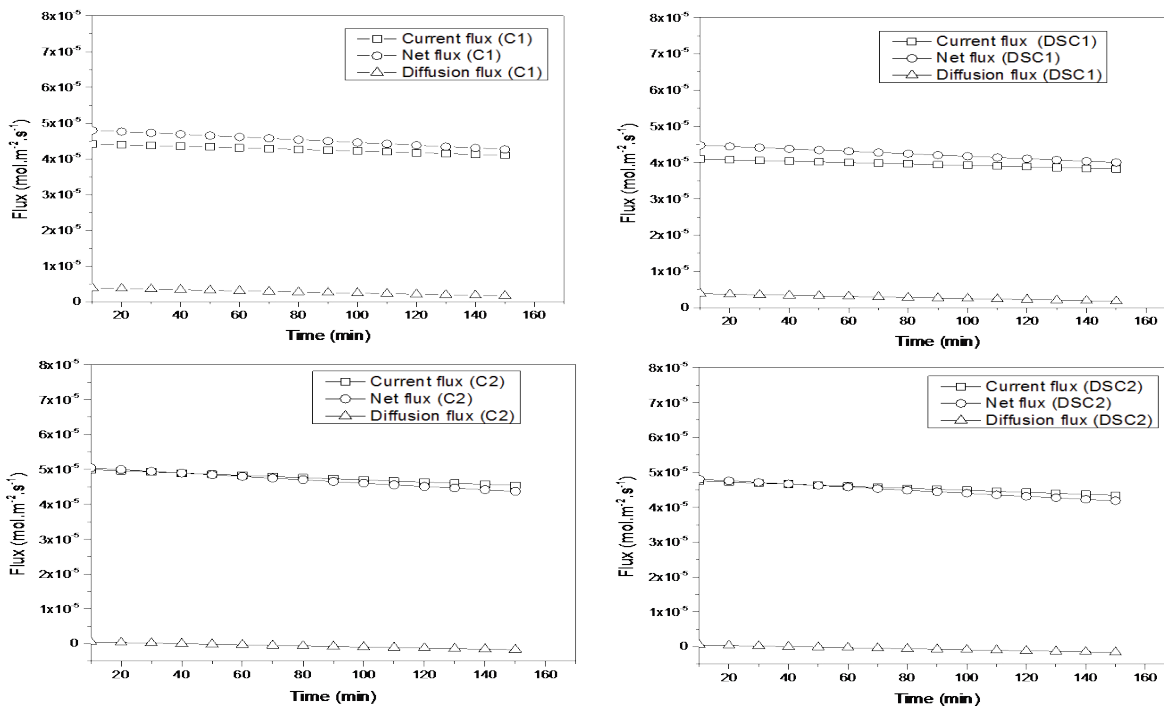
Figure 12: (a): Comparison of current flux, diffusive flux and net flux and their variation with time for experiments C1 - DSC1 and C2 - DSC2.
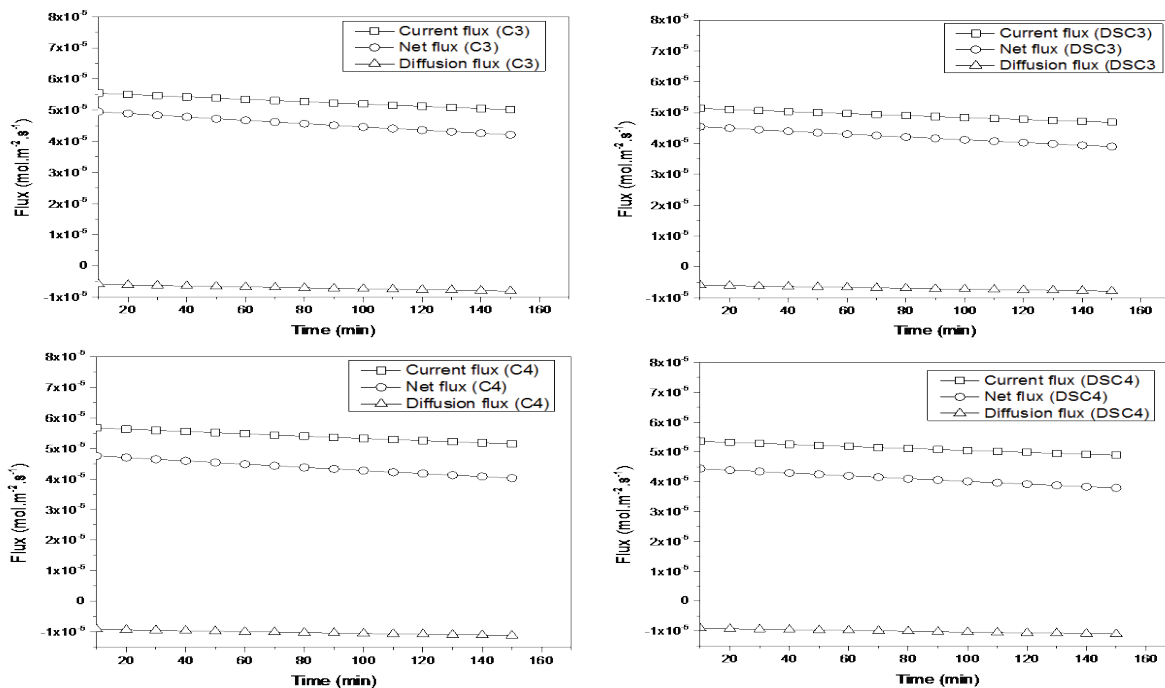

Figure 12: (b): Comparison of current flux, diffusive flux and net flux and their variation with time for experiments C3 – DSC3 and C4 – DSC4.
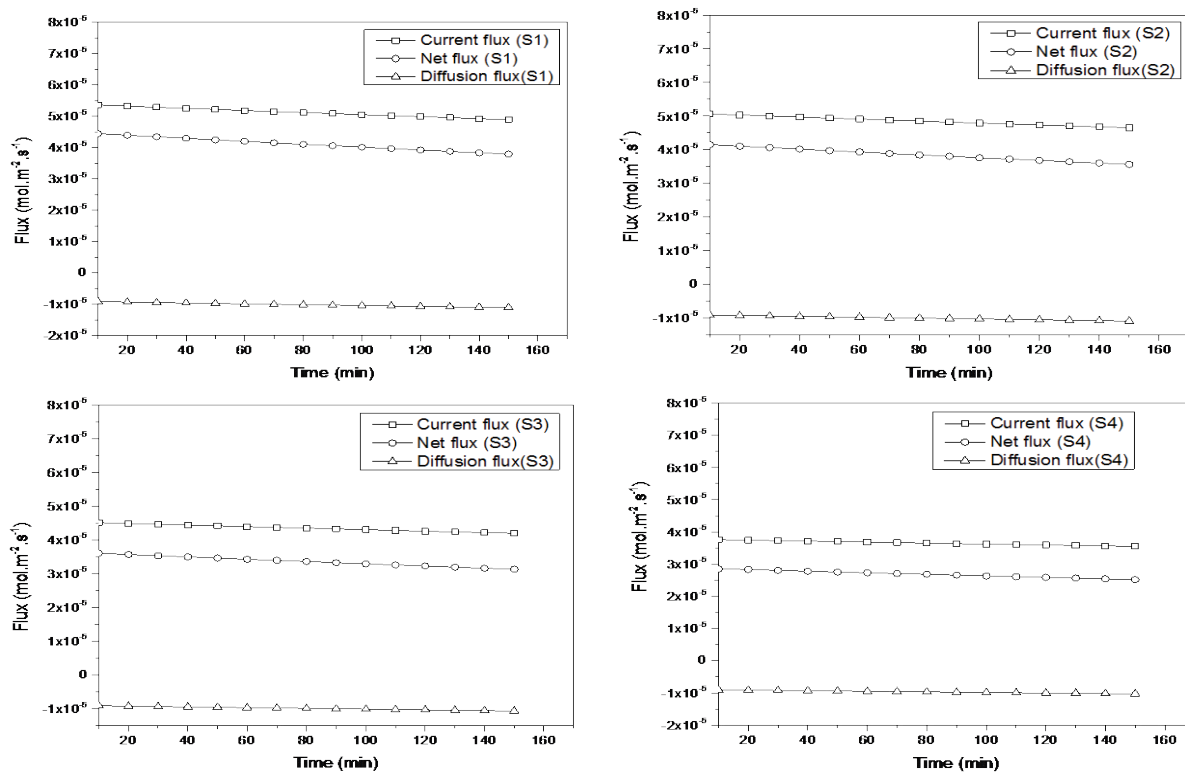
Figure 12: (c): Comparison of current flux, diffusive flux and net flux and their variation with time for experiments C5 – DSC5 and C6 – DSC6.

Investigation on role of sugar concentration in ion removal

Effect of sugar concentration of diluate channel on (i) current density (Figure 10), (ii) concentrate concentration variation (Figure 10), (iii) Ion removal rate (Figure 11) and (iv) net flux Figures 12(d) were experimentally found out.

With increase in sugar concentration the current density drops (Figure 10) thus, current density is maximum with 5% sugar and minimum with 20% sugar and slowly it decreases with time. Gradual lowering in current density between 5% - 20% sugar (S1-S4) may be due to increase in solution viscosity (Figure 5) and reduction in ion conductivity (Figure 7). Thus, hydrated ions experience more resistance under an applied electric potential. Slow drop in current density with time is due to depletion of ions from diluate channel. Gain in concentrate channel concentration supports ion transport from diluate to concentrate channel. The slope of the line indicating ion accumulation rate in concentrate is highest with 5% sugar (S1) while it is the minimum with 20% (S4) sugar concentration. This is due to increase in solution resistance with non-electrolyte sugar molecules. The percent salt removal from diluate stream (Figure 11) supports above fact indicating drop in ion removal rate with increasing sugar concentration.

Estimation of different flux components e.g. current flux, diffusive flux and net flux are presented in Figure 12d. The current flux decreased with increase in the mass% of sugar i.e. in the order of 5% - 20% (S-S4) and thus, effective flux decreases with sugar mass% (Figure 12d).

It is also interesting to note (Figure 13) the ratio of removal rates with sugar and without sugar remains almost constant with concentrate concentration change. Similar constancy is also noted with viscosity ratios and average current density ratios as well. This is possibly due to impermeable (to sugar molecules) nature of ionic membrane used in electro dialysis. This has been confirmed from UV analysis of the concentrate stream before and after operation (Figure 14). No peak is noticed at 400nm (λ_{max} for sugar). Sugar is not an electrolyte and its role is limited to the diluate channel only. The ratios of removal rates (with and without sugar) can be expressed by a simple power function of viscosity ratios as

$$\frac{percent\ removal_C}{percent\ removal_{DSC}} = \left(\frac{\mu_{DSC}}{\mu_C}\right)^{0.28} \qquad (29)$$

This factor of 0.28~0.3 resembles close similarity with Sc number in the Sh number correlation, indicating that the removal rate is a strong function of flow and physical properties of the system.

Mass transfer coefficient and specific energy

Local mass transfer coefficients of ions (cation/anion) and specific energy consumption were estimated using Eqs. (12) and (28) respectively and reported in Figure 15. Mass transfer coefficient directly relates the speed of ion transport phenomena and is a strong function of local parameters of the system. Figure 15 shows local mass transfer coefficients 'k' are always higher with non-sugar cases than those with sugar ones. Presence of non-electrolyte (sugar) reduces mass transfer coefficient and increases overall specific energy consumption to execute a desired separation. Experiments C1 and DSC1 are more energy efficient having lowermost specific energy consumption estimates. Favorable diffusional flux and low current values for these sets (C1, DSC1) probably encourage reduction in energy consumption.
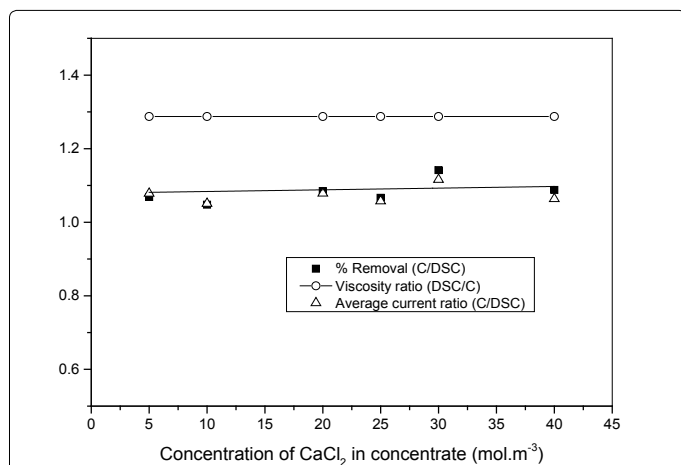
Figure 13: The ratios of % removal (non-sugar/sugar), average current density (non-sugar/sugar) and viscosity (sugar/non-sugar) with change in concentrate concentration.
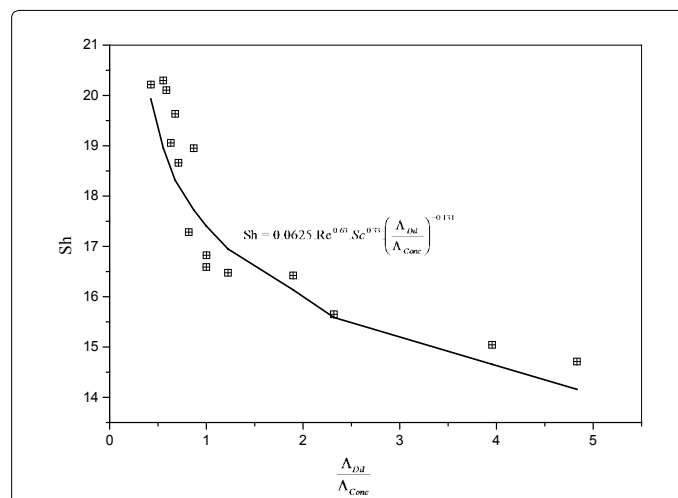

Figure 16: Plot of Sherwood number vs. conductivity ratio of diluate and concentrate to validate the proposed empirical equation (Eq. 21).
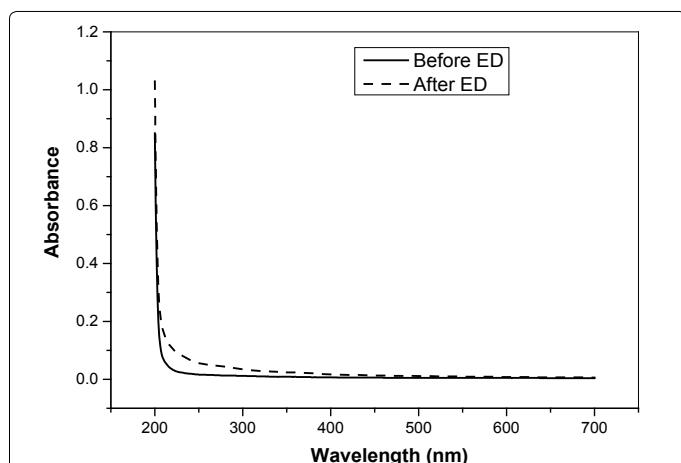
Conclusion

Removal of CaCl₂ from 5% sugar solution was carried out in batch recirculation electrodialysis mode. All experiments, were performed below LCD to avoid water electrolysis. Role of electrolyte concentration in concentrate channel, sugar mass% in diluate stream in ion removal were evaluated. Concentrate concentration variation doesn't follow any trend to predict ion removal rate. Presence of sugar (in the diluate stream) increases the solution viscosity, reduces ion diffusivity and electrical conductivity thus, lowers ion removal rate compared to those without sugar cases. The linearized Nernst-Plank equation efficiently predicted the experimental data and was extensively used to calculate various fluxes (current, diffusional and net), mass transfer coefficients for ions, specific energy consumption. Increase in concentrate concentration reduced overall cell resistance causing higher current density. Diffusional flux plays a major role in deciding overall or net flux. The experiments C1, C2, DSC1 and DSC2 showed favorable diffusional flux and higher ion removal rate with simultaneous reduction of energy consumption. Therefore, an optimum electrolyte concentration of concentrate, sugar mass% in diluate, and applied external electric potential can be obtained from this apparatus Figure 16.

Acknowledgement

References

1. Mathur RBL (1978) Handbook of Cane Sugar Technology. Oxford and IBH Publishing Co New Delhi.

2. Smagghe F, Mourgues J, Escudier JL, Conte T, Molinier J, et al. (1992) Recovery of Calcium Tartrate and Calcium Malate in Effluents from Grape Sugar Production by Electrodialysis. Bioresource Technology 39: 185-189

3. Elmidaoui A, Chay L, Tahaikt M, Sahli MAM, Taky M, et al. (2004) Demineralisation of beet sugar syrup, juice and molasses using an electrodialysis pilot plant to reduce melassigenic ions. Desalination 165: 435.

4. Tragardh G, Gekas V (1988) Membrane Technology in the Sugar Industry. Desalination 69: 9-17

5. Geraldes V, Afonso M D (2010) Limiting current density in the electrodialysis of multi-ionic solutions. J Membr Sci 360: 499-508

6. Lee HJ, Strathmann H, Moon SH (2006) Determination Of The Limiting Current Density In Electro-Dialysis Desalination As An Empirical Function Of Linear Velocity. Desalination 190: 43-50

Figure 14: UV absorption of concentrate stream of S1 before and after electro dialysis. Absence of sugar peak (Wavelength, λ=400 nm) ensures the impermeability of sugar molecules through ion exchange membranes.
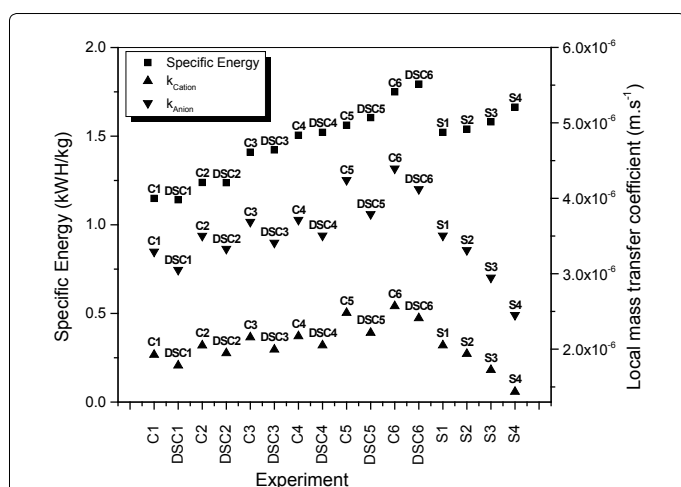

Figure 15: Local mass transfer coefficients of cations, anions and specific energy estimates for experiments C1-C6, DSC1-DSC6 and S1-S4.

7. Tanaka Y (2005) Limiting Current Density of an Ion-Exchange Membrane and of an ElectroDialyzer. J Membr Sci 266: 6-17

8. Strathmann H (2004) Ion-Exchange Membrane Separation Processes. Elsevier

9. Elmidaoui A, Lutin F, Chay L, Taky M, Tahaikt M, et al. (2002) Removal of melassigenic ions for beet sugar syrups by electrodialysis using a new anion-exchange membrane. Desalination 148: 143-148.

10. Krol JJ, Wessking M, Strathmann H (1999) Concentration polarization with monopolar ion exchange membranes: current-voltage curves and water dissociation. J Membr Sci 162: 145-154.

11. Strathmann H, Krol JJ, Rapp HJ, Eigenberger G (1997) Limiting current density and water dissociation in bipolar membranes. J Membr Sci 125: 123-142

12. Ortiz JM, Sotoca JA, Exposito E, Gallud F, Garcia-Garcia V, et al. (2005) Brackish water desalination by electrodialysis: batch recirculation operation modeling. J Membr Sci 252: 65-75

13. Rohman FS, Othman MR, Aziz N (2010) Modeling of batch electrodialysis for hydrochloric acid recovery. Chem Eng J 162: 466-479

14. Fidaleo M, Moresi M (2010) Application of the Nernst-Planck approach to model the electrodialytic recovery of disodium itaconate. J Membr Sci 349: 393-404

15. Fidaleo M, Moresi M (2005) Modeling of sodium acetate recovery from aqueous solutions by electrodialysis. Biotechnol Bioeng 91: 556-568

16. Wen T, Solt GS, Gao DW (1996) Electrical resistance and coulomb efficiency of electrodialysis (ED) apparatus in polarization. J Membr Sci 114: 255-262

17. Tanaka Y (2005) Irreversible thermodynamics and overall mass transport in ion-exchange membrane electrodialysis. J Membr Sci 281: 517-531

18. Kabay N, Demircioglu M, Ersoz E, Kurucaovali I (2002) Removal of calcium and magnesium hardness by electrodialysis. Desalination 149: 343-349

19. Bird RB, Stewart WE, Lightfoot EN (2002) Transport Phenomenon. John Wiley & Sons.

20. Treybal RE Mass-Transfer Operations. McGraw-Hill publications.

21. Balster J, Yildirim MH, Stamatialis DF, Ibanez R, Lammertink RG, et al. (2007) Morphology and microtopology of cation-exchange polymers and the origin of the overlimiting current. J Phys Chem B 111: 2152-2165.

22. Mischuk NA (1998) Perspective of electrodialysis intensification. Desalination 117: 283-296

23. Grigorchuk OV, Vasileva VI, Shaposhnik VA (2005) Local characteristics of mass transfer under electrodialysis demineralization. Desalination 184: 431-438

24. Isaacson MS, Sonin AA (1976) Sherwood Number and Friction Factor correlations for clectrodialysis systems, with application to process optimization. Ind Eng Chem Process Des Dev 15: 313-321

25. Poling BE, Prausnitz JM, O'Connell JP, The Properties of Gases and Liquids. McGraw-Hill publications

26. Li YH, Gregory S (1974) Diffusion of ions in sea water and in deep sea sediments. Geochimica et Comochimics acta 28: 703-714

27. Barragan VM, Ruiz-Bauza C (1998) Current-Voltage Curves for Ion-Exchange Membranes: A Method for Determining the Limiting Current Density. J Colloid Interface Sci 205: 365-373.

28. Koryta J, Dvorak J, Kavan L (1993) Principles of electrochemistry. John Wiley & Sons, Inc.

29. Nwal Amang D, Alexandrova S, Schaetzel P (2003) The determination of diffusion coefficients of counter ion in an ion exchange membrane using electrical conductivity measurement. Electrochimica Acta 48: 2563-2569